RESEARCH

Identification of 17 novel epigenetic biomarkers associated with anxiety disorders using differential methylation analysis followed by machine learning-based validation

Yoonsung Kwon[1,2], Asta Blazyte[1,3], Yeonsu Jeon[4], Yeo Jin Kim[4], Kyungwhan An[1,2], Sungwon Jeon[4,7,8], Hyojung Ryu[4], Dong-Hyun Shin[1,2], Jihye Ahn[4], Hyojin Um[4], Younghui Kang[4], Hyebin Bak[4], Byoung-Chul Kim[4], Semin Lee[1,2], Hyung-Tae Jung[5*], Eun-Seok Shin[6*] and Jong Bhak[1,2,4,7*]

Abstract

Background The changes in DNA methylation patterns may reflect both physical and mental well-being, the latter being a relatively unexplored avenue in terms of clinical utility for psychiatric disorders. In this study, our objective was to identify the methylation-based biomarkers for anxiety disorders and subsequently validate their reliability.

Methods A comparative differential methylation analysis was performed on whole blood samples from 94 anxiety disorder patients and 296 control samples using targeted bisulfite sequencing. Subsequent validation of identified biomarkers employed an artificial intelligence-based risk prediction models: a linear calculation-based methylation risk score model and two tree-based machine learning models: Random Forest and XGBoost.

Results Seventeen novel epigenetic methylation biomarkers were identified to be associated with anxiety disorders. These biomarkers were predominantly localized near CpG islands, and they were associated with two distinct biological processes: 1) cell apoptosis and mitochondrial dysfunction and 2) the regulation of neurosignaling. We further developed a robust diagnostic risk prediction system to classify anxiety disorders from healthy controls using the 17 biomarkers. Machine learning validation confirmed the robustness of our biomarker set, with XGBoost as the best-performing algorithm, an area under the curve of 0.876.

Conclusion Our findings support the potential of blood liquid biopsy in enhancing the clinical utility of anxiety disorder diagnostics. This unique set of epigenetic biomarkers holds the potential for early diagnosis, prediction of treatment efficacy, continuous monitoring, health screening, and the delivery of personalized therapeutic interventions for individuals affected by anxiety disorders.

Keywords Anxiety disorder, Methylation risk score, Machine learning, Epigenetic biomarker, Liquid biopsy

*Correspondence:
Hyung-Tae Jung
lukie004@naver.com
Eun-Seok Shin
sesim1989@gmail.com
Jong Bhak
jongbhak@genomics.org
Full list of author information is available at the end of the article

Kwon *et al. Clinical Epigenetics*   (2025) 17:24

Page 2 of 13

Background

Anxiety disorders, with a global prevalence of approximately 4%, have a higher prevalence compared to other mental disorders [1]. Despite their high prevalence, anxiety disorders are challenging in many regards: diagnosis, primary care, treatment effectiveness monitoring, and relapse prevention [2]. These diverse challenges stem from the difficulty of accurately measuring the state of mental health in individuals, given that mental disorders arise from the complex interplay of genetic and environmental factors, making it challenging with conventional techniques [3]. A twin study suggested that environmental factors may account for up to 12% of clinical variance in anxiety disorders [3]. Moreover, traditional diagnostic methods relying on questionnaires may exhibit variability contingent upon the subject's health status or mood during assessment, underscoring the imperative for complementary approaches [4, 5]. These insights highlight the need for novel approaches to directly measure these complicated effects from molecular materials derived from the patient, circumventing biases that standard clinical diagnostic questionnaires and interviews are prone to.

Recent genomic studies for anxiety disorders, although not reaching any definitive conclusions yet, have yielded a range of diverse biomarkers from various tissues. For example, Edelmann et al. investigated the blood transcriptome and identified 13 significantly differentially expressed genes (DEGs) between individuals diagnosed with social anxiety disorder and healthy controls [6]. Levey et al. reported five blood-derived SNPs associated with generalized anxiety disorder 2-item (GAD-2) scale for European Americans and one SNP in African Americans, respectively, [7] while Su et al. identified 26 genes associated with anxiety through a transcriptome-wide association study (TWAS) utilizing multiple brain tissues [8]. Two blood-derived differentially methylated regions (DMRs) had been reported in association with social anxiety disorder by Wiegand et al. in 2020 [9]. Furthermore, in 2023, an epigenome-wide association study (EWAS) was conducted on the methylation patterns of

anxiety disorder patients based on their blood cell types [10]. However, prior studies faced critical limitations in validating identified biomarkers, as well as lacked dedicated research exploring their application in diagnostic scenarios.

In order to attain a comprehensive understanding of anxiety disorders, which are influenced by a combination of genetic and environmental factors, the utilization of epigenetic data reflecting long-term environmental influences is critical [11, 12]. An efficient approach in this regard involves the assessment of DNA methylation changes in readily accessible tissues, such as blood, for diagnostic purposes. This approach facilitates the integration of epigenetic insights into clinical practice, thus offering valuable insights into the underlying molecular mechanisms and potential diagnostic and therapeutic strategies for anxiety disorders.

This study shows potential for employing peripheral blood and molecular diagnostics in diagnosing anxiety disorders. Bootstrapping techniques were used to identify precise methylation biomarkers in 94 Korean patients diagnosed with anxiety disorders by physicians. Following this, we developed machine learning models to validate the diagnostic capabilities of these biomarkers, assessing their performance in classifying cases from controls in the validation set.

Methods

Study population

A total of 94 patients with anxiety disorder from the Ulsan Medical Center, Ulsan, Korea, were enrolled in this study, and 296 healthy individuals from the Korean Genome Project (KGP) were selected as controls [13, 14]. The healthy control group was configured to match the sex and age distribution of the anxiety patient group (Table 1). All of our anxiety disorder patients received their diagnosis from a psychiatric specialist in a clinical setting. All samples used in our study are presumed to be ethnically Koreans. Information regarding the KGP data

Table 1 Baseline characteristics in this study

		Anxiety disorder patient (n = 94)	Healthy control (n = 296)	*p*-value
Sex	Male	41 (43.62%)	134 (45.27%)	0.813
	Female	53 (56.38%)	162 (54.73%)	
Age		42.98 (15.64)	40.40 (15.76)	0.168
Type of anxiety disorder	Panic disorder	10 (10.64%)	0	NA
	Social anxiety disorder	6 (6.38%)	0	
	Generalized anxiety disorder	78 (82.98%)	0	

Continuous values are represented as mean (standard deviation). Proportions are shown as absolute number (percentage). The following statistical methods were applied: (Sex: Fisher's exact test, Age: Student's t-test, Type of anxiety disorder: Chi-square test). NA = Not Available

can be found on the Korean Genome Project webpage (http://koreangenome.org).

Study design

This study was performed to discover and validate differential methylation biomarkers between anxiety disorder patients and healthy controls (Table 1), employing a machine learning-based approach (Fig. 1). The entire dataset was divided into a discovery set and a validation set, ensuring even distribution of sex, age, and types of anxiety disorders in each set (Additional file 3: Table S1). Moreover, exclusive reliance on the training set was employed in the biomarker discovery process to mitigate overfitting concerns in feature selection.

Targeted bisulfite sequencing and raw data processing

Blood samples were collected in EDTA tubes at the time of recruitment and then frozen, and genomic DNA was extracted using the DNeasy Blood and Tissue Kit from Qiagen (Qiagen, 69,506), following the manufacturer's protocol. The library preparation process followed the protocol of the SureSelectXT Methyl-Seq Target Enrichment System Kit (Agilent, G9651). Then, sequencing was performed using both the Illumina NovaSeq 6000 platform and the Hiseq 2500 platforms, generating paired-end reads of 150 bp and 100 bp, respectively. The adapter trimming process for the sequenced reads was performed using the fastp (version 0.23.1) with specific parameters (thread=16, trim_front1=15, trim_front2=15, trim_tail1=5, trim_tail2=5, length_required=0, cut_front=1, cut_tail=1, cut_right=0, cut_mean_quality=20, average_qual=20, n_base_limit=1, detect_adatper_for_pe) [15, 16]. To analyze the results of bisulfite sequencing, we utilized Bismark (version 0.23.1) with Bowtie2 (version 2.5.1) to align the bisulfite-treated reads to the reference genome (hg38) without scaffolds [17, 18]. We applied the parameters "–L 20 -N 1 -p 10 -q –phred33_quals –dovetail" during the alignment process. Methylation calling for CpG sites was then performed with Bismark (version 0.23.1) [17].

Identification of methylation biomarkers for anxiety disorders

We used the methylKit package (R version 4.1.3; methylKit version 1.20.0) to identify methylation biomarkers in individuals with anxiety disorders [19, 20]. For each CpG site, if the sequencing depth was less than 10, it was treated as NA (not available). 862,525 CpG sites with values present in all samples were utilized for the analysis. In order to identify methylation biomarkers able to
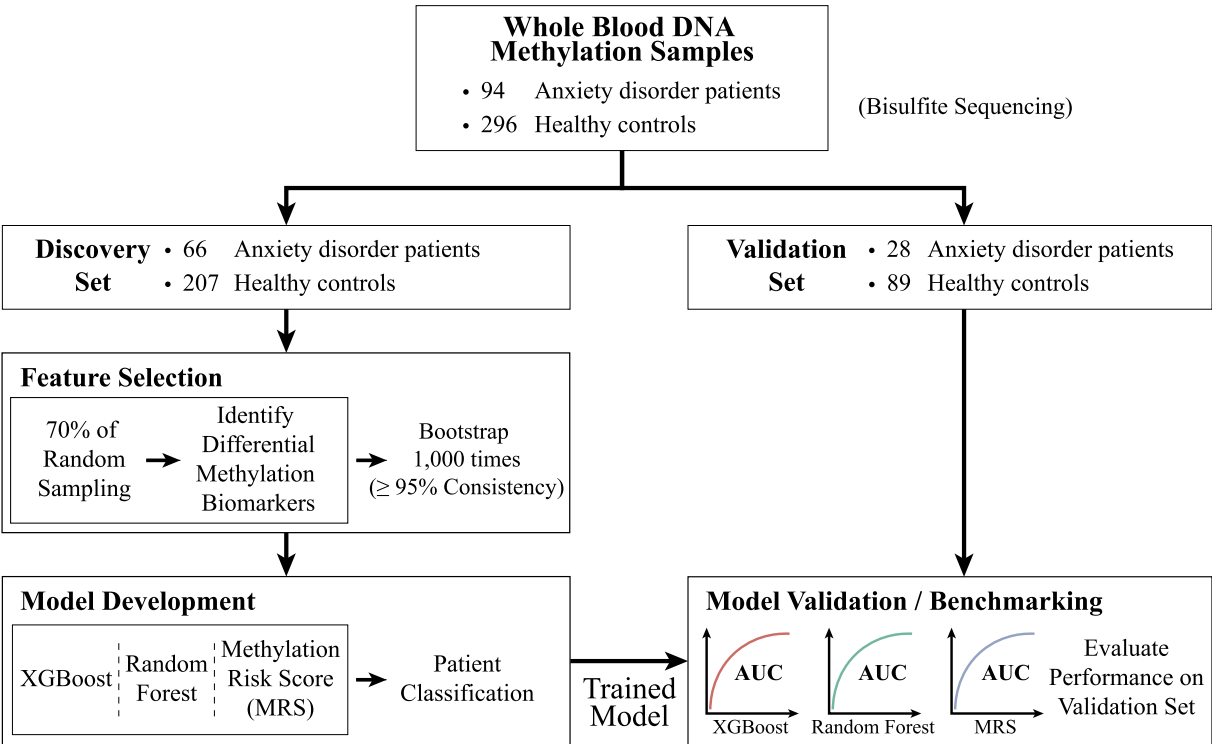

Fig. 1 Study design for the discovery and validation of differentially methylated biomarkers for anxiety disorders. The flow chart illustrates the utilization of methylation data according to the flow of arrows. AUC = Area Under Curve

Kwon *et al. Clinical Epigenetics*   (2025) 17:24

Page 4 of 13

distinguish healthy controls from patients with anxiety disorders, a logistic regression was conducted using the methylKit package, incorporating sex and age as covariates. Furthermore, overdispersion correction was utilized to enhance the precision of the biomarkers, removing false positives [21]. Significant biomarkers were identified using a false discovery rate (FDR; Benjamini–Hochberg correction)-adjusted *p*-value cutoff of 0.05 and at least 10% of mean difference in methylation between patient and control groups in DNA methylation as the threshold.

Establishment of a robust biomarker set through random sampling

A 70% random sampling within the discovery set was conducted 1,000 times to mitigate potential bias due to the reduced discovery set size. Subsequently, we performed methylation biomarker discovery for 1,000 times using the previously outlined methods. Biomarkers that consistently appeared in 95% or more instances across the 1,000 independent analyses were considered robust and eligible for further study. To optimize the biomarker set, we applied various thresholds for the reproducibility rate in the 1,000 biomarker discovery iterations (95%, 96%, 97%, 98%, 99%, and 100%) (Additional file 2: Fig. S1A, and S1B).

Calculation of methylation risk score for anxiety disorders

To assess the performance of the biomarkers identified in the discovery set, we calculated the methylation risk score (MRS) as an indicator for classifying anxiety disorder patients and healthy controls in the validation set. In the MRS calculation, logistic regression [1] was conducted on the discovery set to determine the weight(w_i^{CpG}) of each i-th biomarker as follows:

$$Logit(Y) \sim w_i^{\text{Intercept}} + w_i^{CpG}\beta_{i,\text{Discovery}}$$
$$+ w_i^{\text{Age}}\text{Age}_{\text{Discovery}} + w_i^{\text{Sex}}\text{Sex}_{\text{Discovery}} \qquad (1)$$

where Y corresponds to the condition (healthy control: 0, anxiety disorder patient: 1), Age and Sex the covariates of age and sex for each sample in the discovery set, β the methylation value of the i-th biomarker for the discovery set, w the coefficient for each variable.

$$MRS_j = \sum_{i=1}^{n} w_i^{CpG}\beta_{ij,\text{Validation}} \ (2)$$

For each sample j, the MRS encompassing the entire set of n methylation biomarkers was computed by iteratively multiplying the coefficient and methylation value (β_{ij}) derived from the logistic regression model for each i-th CpG site and subsequently summing these products [2]. The MRS formula was applied to the validation set for

the validation of methylation biomarkers. Subsequently, the performance of the MRS was evaluated by analyzing ROC (receiver operating characteristic) curves.

Application of machine learning models based on differential DNA methylation

The Random Forest model was trained using the Sci-kit learn package (version 0.23.2), and the XGBoost model was trained using the xgboost package (version 1.6.2). Hyperparameter tuning was conducted using the Grid-SearchCV package with cross-validation, targeting relevant parameters for both Random Forest and XGBoost models. For XGBoost, the parameters were max_depth, min_child_weight, gamma, subsample, colsample_bytree, and n_estimators. For Random Forest, the parameters included max_depth, min_samples_split, min_samples_leaf, and n_estimators. Hyperparameter tuning was performed within the validation set and conducted separately for each biomarker set determined by different reproducibility thresholds in random sampling. The tuning process was as follows: 1) All hyperparameters were initially tuned using threefold cross-validation to set initial values. 2) Starting from these initial values, each hyperparameter was tuned one by one through threefold cross-validation in the following order (XGBoost: max_depth, min_child_weight, gamma, subsample, colsample_bytree, and n_estimators; Random Forest: max_depth, min_samples_split, min_samples_leaf, and n_estimators).

Each time a hyperparameter was tuned, the determined optimal value was fixed, and the next hyperparameter was tuned until all hyperparameters were optimized. This process was completed for both XGBoost (tuned optimal hyperparameters; Additional file 4: Table S2) and Random Forest models (tuned optimal hyperparameters; Additional file 5: Table S3) for each biomarker set. To compute the feature importance of each biomarker in the model, we calculated the SHapley Additive exPlanations (SHAP) using the shap package (version 0.41.0) [22]. The entire procedure was carried out in a Python 3.7.16 environment.

Annotation of methylation biomarkers

We annotated the differentially methylated sites (DMSs) using Annotatr (R version 4.1.3; Annotatr version 1.20.0) [23], utilizing the options "hg38_cpgs," "hg38_basicgenes," and "hg38_enhancers_fantom" for the annotation of each CpG site. If a particular CpG site was associated with the location of more than two genes, only those genes related to the promoter region were annotated. Utilizing the ClueGO plug-in (version 2.5.9) [24] in Cytoscape (version 3.9.1), we conducted functional enrichment analysis in Gene Ontology (GO, http://geneontology.org/) [25,

Kwon *et al. Clinical Epigenetics*   (2025) 17:24

Page 5 of 13

26] and Kyoto Encyclopedia of Genes and Genomes (KEGG, https://www.genome.jp/kegg/) [27–29]. The *p*-values from the enrichment test underwent correction using the Benjamini–Hochberg method to calculate the false discovery rate (FDR). We identified statistically significant entries based on the criterion of FDR < 0.05.

Statistical analysis

All the statistical analyses were performed using the SciPy package (version 1.7.3) in Python (version 3.7.16). Fisher's exact test assessed the difference in sex ratio between healthy control and anxiety disorder patients, while Student's t-test examined the difference in age distribution between them. To verify the equivalent stratification of samples during the discovery-validation splitting, the Chi-square test checked the distribution of the type of anxiety disorder among anxiety disorder patients in the discovery set and validation set. Furthermore, Fisher's exact test and Student's t-test were applied to evaluate the distribution of each sex and age between the discovery set and the validation set.

Results

Detecting differentially methylated sites and classification model construction

Employing bootstrapping on the discovery set to maximize the robustness, we identified 18 methylation biomarkers (Fig. 2A and Additional file 6: Table S4) that showed significantly different methylation values with over 95% reproducibility out of 1,000 biomarker discoveries (Additional file 2: Fig. S1A-C) between 66 anxiety disorder patients and 207 healthy controls (Fig. 1). The optimal marker set, however, consisted of 17 markers that exhibited a reproducibility of at least 97% (Fig. 2B), reflecting the consistency in marker discovery during bootstrapping (Additional file 2: Fig. S1A, and S1B). Of these, 16 were hypomethylated biomarkers, and one (CpG site located in the intronic region of the *INPP5A* gene) was hypermethylated. Although these biomarkers were discovered in the discovery set, they were also significantly different between anxiety disorder patients and healthy controls in the validation set (17 markers p-value < 0.05 on both discovery set and validation set; Additional file 2: Fig. S1D-F). Importantly, these 17 biomarkers retained their significance even after adjusting for additional covariates such as current smoking and alcohol consumption (Additional file 2: Fig. S2A) and showed no association with antidepressant medication use (FDR > 0.05) (Additional file 2: Fig. S2B). These results suggest that the identified biomarkers reflect the intrinsic characteristics of the disease itself rather than being influenced by other disease-related confounders.

To evaluate the discriminatory power of 18 methylation biomarkers in the validation set, comprising 28 anxiety disorder patients and 89 healthy controls (Fig. 1), three primary approaches were employed: a linear calculation-based MRS model and two tree-based machine learning models (Random Forest and XGBoost). Overall, all models demonstrated high performance with AUROC (Area under the receiver operating characteristic curve) above 0.8 (Fig. 2D). In the MRS model, the performance differences across biomarker sets (subsampled from the 18 identified putative biomarkers based on their reproducibility) were relatively consistent (standard deviation of AUROC for MRS: 0.0058), while machine learning-based models exhibited more considerable variations (standard deviation of AUROC for Random Forest: 0.0253, XGBoost: 0.0197) (Additional file 2: Fig. S3C). The average performance, ranked from highest to lowest based on AUROC, was observed as follows: Random Forest, XGBoost, and MRS (mean AUROC of Random Forest: 0.8524, XGBoost: 0.8521, and MRS: 0.8466). The overall high performance of these models indicates the robustness of the markers identified in this study in classifying anxiety disorders, regardless of the method used.

This marker set was further optimized using the best-performing model, XGBoost, with multiple reproducibility thresholds and yielded an even more robust 17 biomarker set. Subsequently, training the XGBoost model with 17 markers exhibiting a reproducibility of 97% or higher based on AUROC values yielded the highest performance (AUROC: 0.876, AUPRC: 0.654, sensitivity: 96.429%, specificity: 67.416%) (AUPRC; Additional file 2: Fig. S3A, and S3B). This model demonstrated the highest performance compared to previous models for classifying anxiety disorder patients based on electronic health check-up records (AUROC: 0.73, sensitivity: 66%, specificity: 70%) [30], brain gray matter volumes in adolescents (AUROC: 0.63) [31], or the DASS-21 (The Depression, Anxiety and Stress Scale—21 Items) questionnaire (73.3% accuarcy on naïve Bayes model) [32]. In this final model, we calculated the feature importance of each biomarker using SHapley Additive exPlanation (SHAP) values, which revealed the only hypermethylated CpG site, located in the intronic region of the *INPP5A* gene, had the highest importance (SHAP = 0.5658), followed by the hypo-methylated intergenic CpG site located in between of the *MUTYH* and *TOE1* genes (SHAP = 0.4163) (Fig. 2B).

Majority of 17 methylation biomarkers are located on CpG islands

Seventeen differentially methylated sites (DMSs) were located on the genomic locations of eleven genes (Table 2). Among these, 82.35% (14/17) of CpG sites
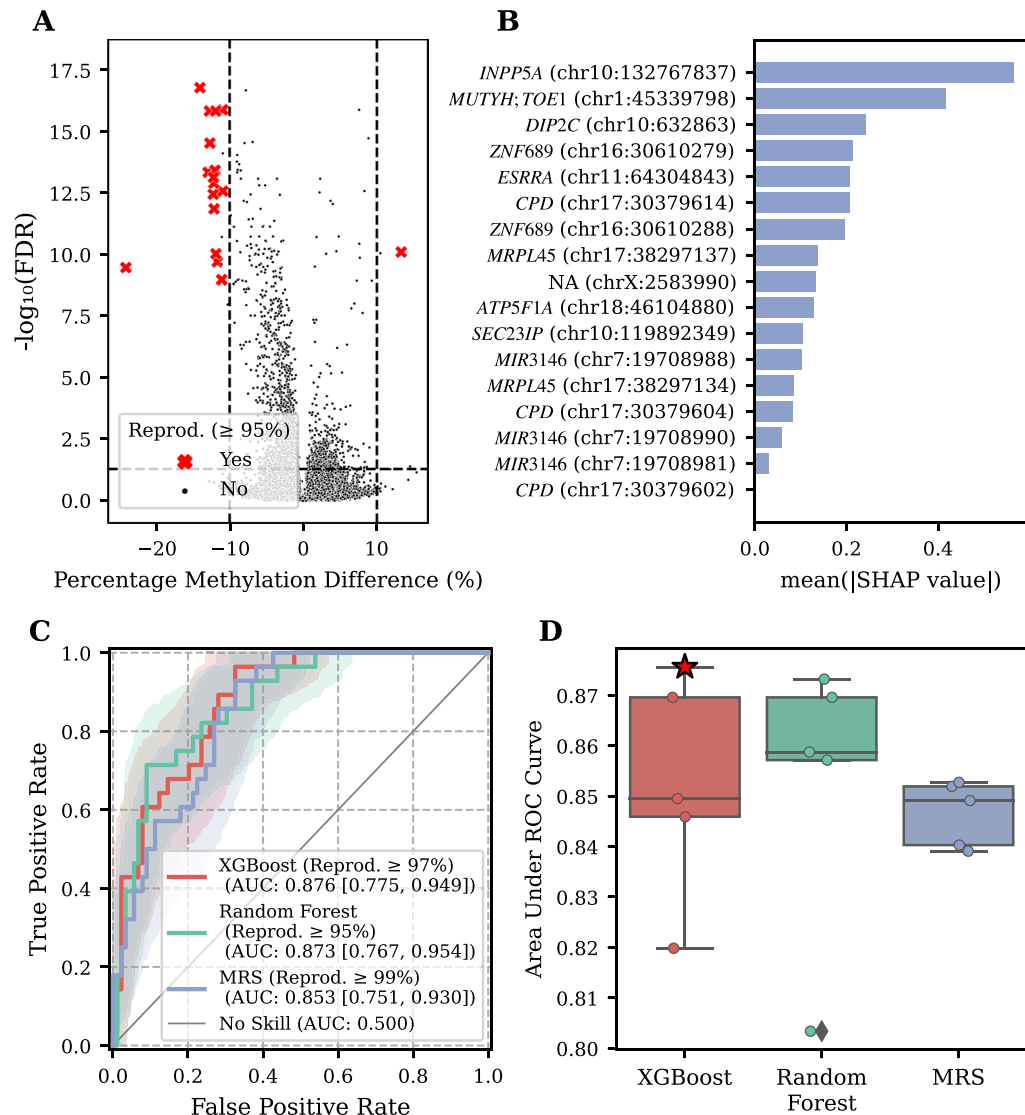
Fig. 2 Discovery of Biomarkers Predictive of Anxiety Disorders and Construction of Classification Model. **A** Volcano plot depicting biomarkers observed in the entire dataset. Biomarkers showing equal to or higher than 95% reproducibility through bootstrapping in the discovery set are highlighted in red. Reprod. = Reproducibility; **B** The feature importance of each biomarker using the best-performing model (XGBoost) on the consensus biomarker set with 97% of reproducibility. The X-axis represents the average impact on the model output magnitude, while the Y-axis depicts the positions of 17 biomarkers showing 97% or higher reproducibility and the associated gene names. If there are two or more genes associated, they are separated by a semicolon. SHAP = SHapley Additive exPlanations; **C** Receiver Operating Characteristic (ROC) curves for each model (XGBoost, Random Forest, and MRS) using the biomarker set that demonstrated the highest performance. The shaded regions indicate the 95% confidence intervals, while the legend displays the area under the ROC curve (AUC) along with its corresponding 95% confidence intervals. Reprod. = Reproducibility; **D** Box plot illustrating the Area Under the ROC curve (AUROC) values for each model (XGBoost, Random Forest, and MRS). Each dot represents the performance of the model for each of the five reproducibility thresholds, and the star indicates the model with the highest performance among all conditions

were located in the promoter regions of genes (including 1~5 kb upstream of the transcription start site as promoter) (Fig. 3, and Table 2). Moreover, 82.35% (14/17) of CpG sites were located within CpG islands (Fig. 3). The other three CpG sites were also located on CpG shores (Fig. 3). All 17 methylation biomarkers identified in this study are located near CpG islands, as CpG shores are defined as 2 kb upstream or downstream of CpG islands. Furthermore, all four regions where DMS biomarkers clustered within 100 bp (*MIR3146*, *ZNF689*, *CPD*, and *MRPL45*) were located within CpG islands (Additional file 2: Fig. S4). This

Table 2 Summary of the 17 CpG site locations, associated genes, and CpG annotations

Chromosome	Position	Gene symbol	Genomic location	Direction of methylation difference	CpG Annotation
chr1	45,339,798	*MUTYH*	Intron; Exon; Far Promoter; 5'UTR; Intron–Exon Boundary	Hypo	CpG Shore
		TOE1	Promoter; Far Promoter		
chr7	19,708,981	*MIR3146*	Far Promoter	Hypo	CpG Island
chr7	19,708,988	*MIR3146*	Far Promoter	Hypo	CpG Island
chr7	19,708,990	*MIR3146*	Far Promoter	Hypo	CpG Island
chr10	632,863	*DIP2C*	Intron	Hypo	CpG Island
chr10	119,892,349	*SEC23IP*	Promoter	Hypo	CpG Shore
chr10	132,767,837	*INPP5A*	Intron	Hyper	CpG Shore
chr11	64,304,843	*ESRRA*	Promoter; Far Promoter	Hypo	CpG Island
chr16	30,610,279	*ZNF689*	Intron; Exon; Promoter; 5'UTR; Intron–Exon Boundary	Hypo	CpG Island
chr16	30,610,288	*ZNF689*	Intron; Exon; Promoter; 5'UTR; Intron–Exon Boundary	Hypo	CpG Island
chr17	30,379,602	*CPD*	Exon; Promoter	Hypo	CpG Island
chr17	30,379,604	*CPD*	Exon; Promoter	Hypo	CpG Island
chr17	30,379,614	*CPD*	Exon; Promoter	Hypo	CpG Island
chr17	38,297,134	*MRPL45*	Exon; Promoter; 5'UTR	Hypo	CpG Island
chr17	38,297,137	*MRPL45*	Exon; Promoter; 5'UTR	Hypo	CpG Island
chr18	46,104,880	*ATP5F1A*	Promoter	Hypo	CpG Island
chrX	2,583,990	NA	NA	Hypo	CpG Island

If a gene associated with a biomarker has annotations for different genomic locations based on transcripts, all genomic locations are listed with semicolons. The direction of methylation difference is indicated as "Hyper" for hypermethylated biomarkers and "Hypo" for hypomethylated biomarkers. NA = Not Available
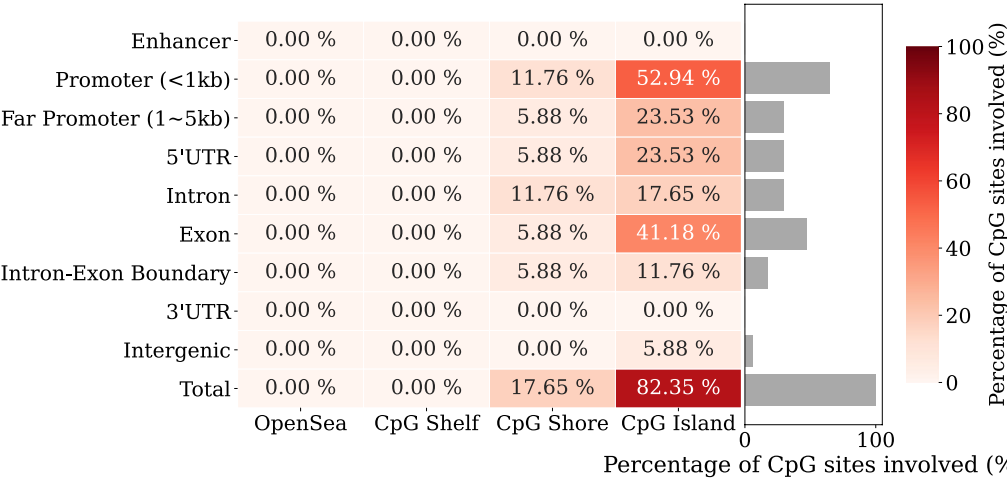

Fig. 3 Summary of the genomic locations of the 17 biomarkers. Heatmap illustrates the frequencies of the 17 biomarkers based on their genomic location. The X-axis represents CpG annotation, while the Y-axis represents genomic annotation of genes. The heatmap colors, as indicated by the color bar on the right, depict the percentage involvement of 17 biomarkers across different CpG annotations and genomic locations. Bar plot shows the percentage of biomarkers in each genomic location

indicates that the biomarkers for anxiety disorders play a significant role in regulating molecular mechanisms within CpG-enriched regions [33–35]. In the pathway enrichment analysis, these eleven genes did not share any significant pathways (Additional file 8: Table S6).

Kwon *et al. Clinical Epigenetics*   (2025) 17:24

Page 8 of 13

The interpretation of eleven genes associated with 17 methylation biomarkers

From the literature search, we found these genes are broadly associated with two main mechanisms: 1) mitochondrial dysfunction and cell apoptosis and 2) the regulation of neurosignaling (Detailed explanation; Additional file 1: Supplementary Text). Five genes (*ATP5F1A*, *INPP5A*, *ESRRA*, *MRPL45*, and *MUTYH*) were related to mitochondrial functions, especially ATP synthesis and the response to Reactive Oxygen Species (ROS) stress (Fig. 4A) [36–43]. Additionally, *ZNF689*, *MIR3146*, and *TOE1* were associated with cell apoptosis through cell
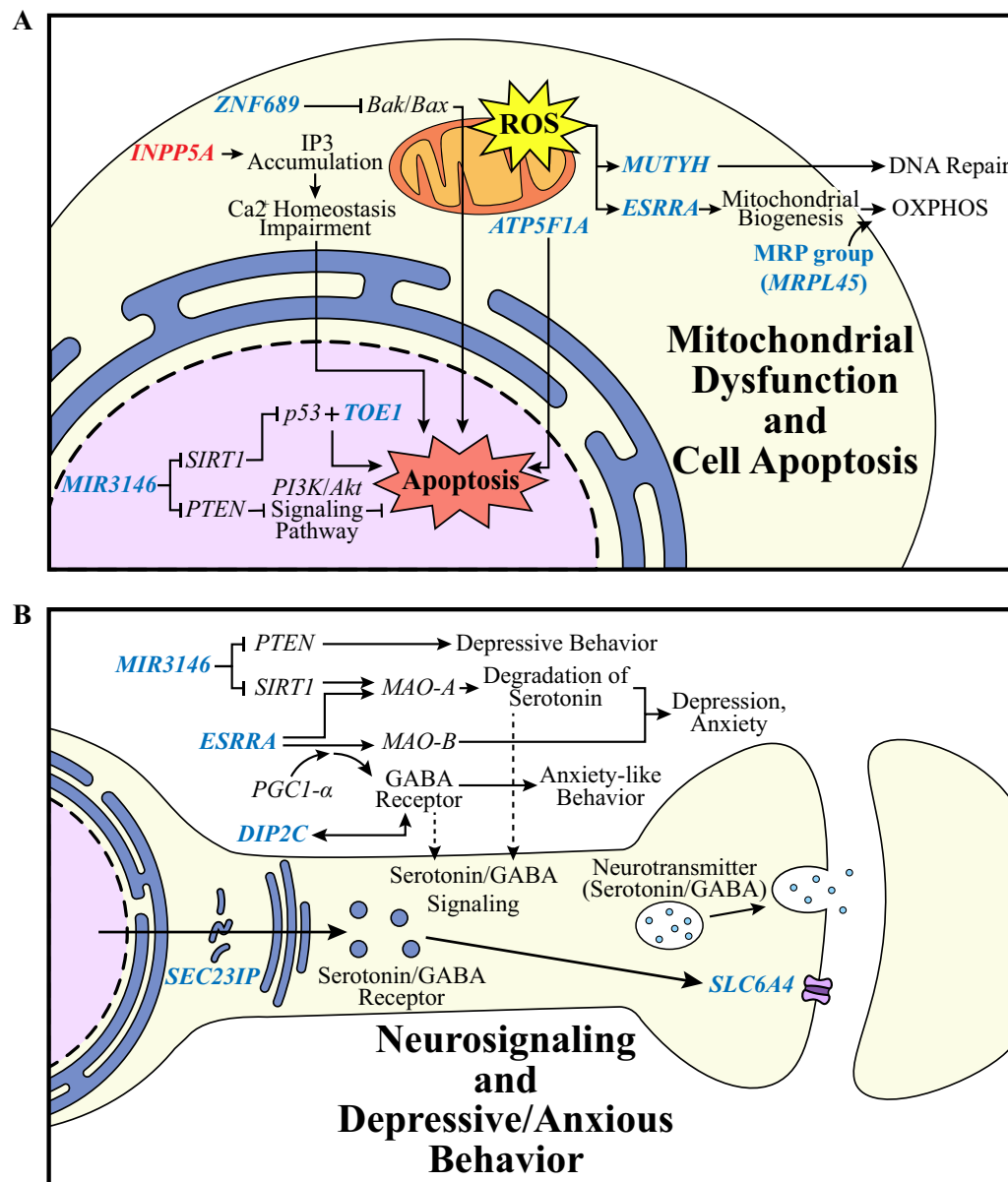

Fig. 4 A diagram representing the molecular pathways of the 17 biomarkers' associated genes. This figure represents the functions of genes in the cellular component and was drawn by the authors. The genes highlighted in blue represent genes identified as hypomethylation biomarkers in our study, while those in red denote genes identified as hypermethylation biomarkers. **A** A chart illustrating the pathways of 8 genes related to mitochondrial dysfunction and cell apoptosis. The functions related to mitochondria and apoptosis are schematically illustrated, with major functions represented by star-shaped speech bubbles. ROS = Reactive Oxygen Species; OXPHOS = Oxidative Phosphorylation; **B** A diagram depicting the pathways of 5 genes associated with serotonin/GABA neurotransmitter signaling and depressive/anxious behavior. The figure illustrates the serotonin/GABA-related pathway within nerve cells, depicting the transport of serotonin/GABA receptors from the endoplasmic reticulum exit site and the transmission of neurotransmitters

Kwon *et al. Clinical Epigenetics*   (2025) 17:24

Page 9 of 13

stress (Fig. 4A) [44–49]. In contrast, five genes (*MIR3146*, *ESRRA*, *SEC23IP*, *DIP2C*, and *CPD*(*SLC6A4*)) were directly related to serotonin and GABA neurotransmitters, which are known to be relevant to mood disorders like depression and anxiety (Fig. 4B) [44, 45, 50–62]. Notably, the genes *MIR3146* and *ESRRA*, identified in this study, exhibit associations with both cell apoptosis and neurosignaling, implying a potential linkage between these two fundamental mechanisms.

This study's identified biomarker in the intronic region of the INPP5A gene (chr10:132,767,837) yields intriguing findings on multiple fronts. Noteworthy for being the sole hypermethylation biomarker among the 17 biomarkers and showcasing a remarkable 99.8% reproducibility (Additional file 6: Table S4), with only two exceptions in 1,000 bootstrapping iterations, this biomarker has previously been linked to cognitive functions [63, 64]. Furthermore, it ranked the highest importance in the XGBoost model (Fig. 2B). Collectively, these pieces of evidence underscore the potentially pivotal role of this gene in the landscape of anxiety disorders.

Discussion

The anxiety patient classification model in our study overcame the limitations of relatively moderate performance observed in previous studies [30–32]. However, this study could not elucidate the specific causal relationships through which these biomarkers manifest uniquely in anxiety disorder patients. Additionally, all participants in this study already had anxiety disorders, making it impossible to determine whether these biomarkers had undergone changes prior to the onset of anxiety disorders. We think continuous monitoring of DNA methylation and clinical changes in individuals who did not have anxiety disorders before their onset can provide insights into the causality of the 17 biomarkers and reveal patterns of change associated with the progression of anxiety disorders.

In this study, three models (XGBoost, Random Forest, and MRS) were utilized to classify anxiety disorder patients. While the machine learning-based models (XGBoost and Random Forest) generally demonstrated higher performance (Fig. 2D), their efficacy varied significantly depending on the combination of marker sets used (Additional file 2: Fig.S3C). Notably, there was a substantial drop in performance when only the four CpG sites that consistently appeared as biomarkers in all 1,000 random sampling iterations were used as features. On the other hand, the MRS model, based on a linear calculation, exhibited lower average performance but showed less variation, even when using a small number of biomarkers. This suggests that MRS could offer consistent performance at a lower cost with fewer

biomarkers in practical clinical applications. Additionally, since MRS involves a simple linear equation, it is easier to understand and does not require the installation of specific machine learning packages for clinical use. These findings highlight the clinical strengths of MRS and suggest that the MRS model is well-suited for practical application in the context of anxiety disorder.

Four out of eleven genes associated with methylation biomarkers have been reported as relevant in previous research [10, 63–70]. In previous studies, the altered methylation patterns of the *INPP5A* gene were associated with cognitive functions in both blood and hippocampus samples [63, 64]. The *DIP2C* gene has been previously reported to undergo changes in its methylation patterns in studies related to anxiety disorder, post-traumatic stress disorder (PTSD), and major depressive disorder [10, 65–68]. Furthermore, despite their distinct genomic positions, both *INPP5A* and *DIP2C* have been identified as markers in a blood-based study for diagnosing anxiety disorders [69]. The methylation and gene expression patterns of the *ATP5F1A* gene are known to be associated with Alzheimer's disease [70]. However, the majority of the genes associated with the remaining DMSs in this study have not previously been documented as undergoing methylation changes related to mental disorders.

It is important to note that previous studies have demonstrated the impact of psychological stress on apoptosis in immune cells within the bloodstream [71–76]. Psychological stress induces cell apoptosis in immune cells, leading to suppression of the immune system and potential development of cancer [73–76]. Additionally, overexpression or knockout of antioxidant enzymes alters oxidative stress levels, which are linked to immune responses and correlate with changes in anxiety-like behavior [71]. Recent studies suggest this may be attributed to the accumulation of oxidized proteins [72]. This study, through the identification of differential methylation in genes associated with cell stress response, regulation of mitochondrial function, and control of apoptosis in individuals with anxiety disorders, provides support for these previous findings. The outcomes presented, along with the predominant localization of CpG biomarkers in CpG island regions observed in our investigation, indicate that the cell apoptosis pattern induced by anxiety disorders can instigate specific molecular alterations in the blood. We suggest this mechanism as a pivotal avenue for detecting anxiety disorders through blood-based assessments.

The association between serotonin, gamma-aminobutyric acid (GABA), and affective disorders has been extensively explored in existing research. Serotonin is a well-known neurotransmitter involved in emotion

Kwon *et al. Clinical Epigenetics*   (2025) 17:24

Page 10 of 13

regulation [77, 78]. GABA, the primary inhibitory transmitter, plays a crucial role in preventing excessive neuronal hyperexcitability through its mutual homeostasis with glutamate [79]. These functions closely link serotonin and GABA with anxiety spectrum disorders, making it a target for antidepressant treatments as well [80, 81]. Interestingly, it is known that when serotonin and GABA are expressed in immune cells, they reduce oxidative stress [82, 83] and regulate cell apoptosis [84, 85]. Additionally, previous studies have shown that serotonin reuptake inhibitors (SSRIs), which are used as antidepressant drugs, reduce the activity of the antioxidant enzyme superoxide dismutase in patients [86]. The detailed mechanisms behind this require further study. In this study, we identified nine biomarkers related to neurotransmitter signaling (Fig. 4B), including four biomarkers associated with two genes (*MIR3146* and *ESRRA*) also involved in cell apoptosis. Although it is unclear whether these findings are related to emotion regulation in the brain or neurotransmitter mechanisms in immune cells, they suggest the possibility that mitochondrial dysfunction/cell apoptosis and neurosignaling pathways are epigenetically co-regulated.

The composition of the anxiety disorder patient sample group in our study is acknowledged as a significant limitation. The relatively small sample size of 94 patients may have impacted the robustness of our findings, particularly during the process of splitting the dataset into the discovery and the validation set for biomarker discovery and validation. Moreover, the use of distinct recruitment sources for patients (Ulsan Medical Center) and controls (Korean Genome Project) posed additional challenges, limiting the feasibility of direct clinical comparisons and comprehensive adjustments for potential confounders. All patients were recruited from a specific hospital in Korea, primarily diagnosed with generalized anxiety disorder (82.98%), with an average age of 42.98 years (standard deviation: 15.64) (Table 1), suggesting a high potential for biased results within a specific population. Given that DNA methylation can vary significantly based on ethnic group or age, recruiting a more diverse and larger sample group could provide a more general understanding of the characteristics of anxiety disorders [87–89].

Conclusions

In our study, we identified and validated 17 novel epigenetic biomarkers associated with anxiety disorders, showing a performance of area under the curve (AUC) of 0.876. These biomarkers were linked to 1) mitochondrial dysfunction and cell apoptosis and 2) the regulation of neurosignaling. Despite the successful validation, this study could not explain the causality associated

with the identified biomarkers in anxiety disorders, and it failed to interpret why biomarkers related to neurosignaling appeared in whole blood samples. Additionally, due to limitations in the anxiety patient dataset, the results in this study have the possibility of biased results toward a specific population. Further recruitment of additional sample cohorts is necessary to address these limitations. Nevertheless, despite these shortcomings, the study underscores the clinical utility of blood liquid biopsy in the diagnosis of anxiety disorders. Furthermore, these biomarkers indicate the potential for early diagnosis, predicting treatment efficacy, continuous monitoring, health screening, and delivering personalized therapeutic interventions for anxiety disorders.

Abbreviations

AUC	Area under curve
AUPRC	Area under the precision-recall curve
AUROC	Area under the receiver operating characteristic curve
CpG site	A region of DNA where a cytosine is followed by a guanine that has the potential to be methylated
DASS-21	The Depression, Anxiety and Stress Scale–21 Items
DEGs	Differentially expressed genes
DMRs	Differentially methylated regions
DMSs	Differentially methylated sites
EWAS	Epigenome-wide association study
FDR	False discovery rate
GABA	Gamma-aminobutyric acid
GAD	Generalized anxiety disorder
GAD-2	Generalized Anxiety Disorder 2-item
GO	Gene Ontology
HC	Healthy control
Hyper	Hypermethylated
Hypo	Hypomethylated
KEGG	Kyoto Encyclopedia of Genes and Genomes
KGP	Korean Genome Project
MRS	Methylation risk score
NA	Not available
OXPHOS	Oxidative Phosphorylation
PD	Panic disorder
PRC	Precision-recall curve
PTSD	Post-traumatic stress disorder
Reprod	Reproducibility
ROC	Receiver operating characteristic
ROS	Reactive oxygen species
SAD	Social anxiety disorder
SHAP	SHapley Additive exPlanations
SSRIs	Serotonin reuptake inhibitors
TWAS	Transcriptome-wide association study

Supplementary Information

Supplementary material 1

Supplementary material 2

Supplementary material 3

Supplementary material 4

Supplementary material 5

Supplementary material 6

Supplementary material 8

Supplementary material 9

Kwon *et al. Clinical Epigenetics*   (2025) 17:24

Page 11 of 13

Author contributions
Conceptualization: S.J., B.K., H.J., E.S., and J.B.; Resources: J.A., H.U., Younghui K., H.B., and H.J.; Data curation: Yoonsung K., A.B., Y.J., Yeo Jin K., D.S., and H.J.; Methodology: Yoonsung K., A.B., Y.J., Yeo Jin K., K.A., S.J., H.R., D.S., E.S., and J.B.; Software, Formal analysis, Visualization, and Validation: Yoonsung K.; Investigation: Yoonsung K., A.B., Y.J., K.A., and D.S.; Funding acquisition: B.K., S.L., H.J., and J.B.; Supervision: S.L., H.J., E.S., and J.B.; Project administration: E.S., and J.B.; Writing-original draft: Yoonsung K., A.B., and D.S.; Writing-review&editing: Y.J., Yeo Jin K., K.A., S.J., H.R., S.L., H.J., E.S., and J.B.; All authors reviewed and approved the final version of the manuscript.

Availability of data and materials
The datasets and materials used in the study are available from the corresponding author upon reasonable request.

Declarations

Ethics approval and consent to participate
Written informed consent was obtained from all participants in this study. Sample collection and sequencing were approved by the Institutional Review Board (IRB) of the Ulsan Medical Center (USH.20.013) and Ulsan National Institute of Science and Technology (UNISTIRB-15–19-A).

Competing interests
Y.J., Yeo Jin K., S.J., H.R., J.A., H.U., Younghui K., H.B., and B.K. are employees, and J.B. is the CEO of Clinomics Inc. S.J. is the CEO of both AgingLab and Geromics. The authors declare no other competing interests.

Author details
[1]Korean Genomics Center (KOGIC), Ulsan National Institute of Science and Technology (UNIST), Ulsan 44919, Republic of Korea. [2]Department of Biomedical Engineering, College of Information and Biotechnology, Ulsan National Institute of Science and Technology (UNIST), Ulsan 44919, Republic of Korea. [3]Lee Gil Ya Cancer and Diabetes Institute, Gachon University, Incheon 406-840, Republic of Korea. [4]Clinomics Inc, Osong 66819, Republic of Korea. [5]Department of Psychiatry, Ulsan Medical Center, Ulsan 44686, Republic of Korea. [6]Department of Cardiology, Ulsan University Hospital, University of Ulsan College of Medicine, Ulsan 44033, Republic of Korea. [7]AgingLab, Ulsan 44919, Republic of Korea. [8]Geromics Inc., Suwon 16226, Republic of Korea.

References
1. Javaid SF, Hashim IJ, Hashim MJ, Stip E, Samad MA, Ahbabi AA. Epidemiology of anxiety disorders: global burden and sociodemographic associations. Middle East Curr Psychiatry. 2023;30(1):44.
2. Bandelow B, Michaelis S, Wedekind D. Treatment of anxiety disorders. Dialogues Clin Neurosci. 2017;19(2):93–107.
3. Hettema JM, Prescott CA, Myers JM, Neale MC, Kendler KS. The structure of genetic and environmental risk factors for anxiety disorders in men and women. Arch Gen Psychiatry. 2005;62(2):182–9.
4. Koerner N, Antony MM, Dugas MJ. Limitations of the hamilton anxiety rating scale as a primary outcome measure in randomized, controlled trials of treatments for generalized anxiety disorder. Am J Psychiatry. 2010;167(1):103–4.
5. Andrews B, Hejdenberg J, Wilding J. Student anxiety and depression: Comparison of questionnaire and interview assessments. J Affect Disord. 2006;95(1):29–34.
6. Edelmann S, Wiegand A, Hentrich T, Pasche S, Schulze-Hentrich JM, Munk MHJ, et al. Blood transcriptome analysis suggests an indirect molecular association of early life adversities and adult social anxiety disorder by immune-related signal transduction. Front Psychiatry. 2023;14:1125553.
7. Levey DF, Gelernter J, Polimanti R, Zhou H, Cheng Z, Aslan M, Quaden R, Concato J, Radhakrishnan K, Bryois J, Sullivan PF, et al. Reproducible genetic risk loci for anxiety: results From ~200,000 participants in the million veteran program. Am J Psychiatry. 2020;177(3):223–32.
8. Su X, Li W, Lv L, Li X, Yang J, Luo XJ, et al. Transcriptome-wide association study provides insights into the genetic component of gene expression in anxiety. Front Genet. 2021;12: 740134.
9. Wiegand A, Kreifelts B, Munk MHJ, Geiselhart N, Ramadori KE, MacIsaac JL, et al. DNA methylation differences associated with social anxiety disorder and early life adversity. Transl Psychiatry. 2021;11(1):104.
10. Hettema JM, van den Oord EJCG, Zhao M, Xie LY, Copeland WE, Penninx BWJH, et al. Methylome-wide association study of anxiety disorders. Mol Psychiatry. 2023;28(8):3484–92.
11. Martin EM, Fry RC. Environmental influences on the epigenome: exposure- associated DNA methylation in human populations. Annu Rev Public Health. 2018;39(1):309–33.
12. Keil KP, Lein PJ. DNA methylation: a mechanism linking environmental chemical exposures to risk of autism spectrum disorders? Environ Epigenetics. 2016;2(1):dvv012.
13. Jeon S, Bhak Y, Choi Y, Jeon Y, Kim S, Jang J, et al. Korean Genome Project: 1094 Korean personal genomes with clinical information. Sci Adv. 2020;6(22):eaaz7835.
14. Jeon Y, Jeon S, Blazyte A, Kim YJ, Lee JJ, Bhak Y, et al. Welfare genome project: A participatory Korean personal genome project with free health check-up and genetic report followed by counseling. Front Genet. 2021;12: 633731. https://doi.org/10.3389/fgene.2021.633731.
15. Chen S, Zhou Y, Chen Y, Gu J. fastp: an ultra-fast all-in-one FASTQ preprocessor. Bioinformatics. 2018;34(17):i884–90.
16. Chen S. Ultrafast one-pass FASTQ data preprocessing, quality control, and deduplication using fastp. iMeta. 2023;2(2):e107.
17. Krueger F, Andrews SR. Bismark: a flexible aligner and methylation caller for Bisulfite-Seq applications. Bioinformatics. 2011;27(11):1571–2.
18. Langmead B, Salzberg SL. Fast gapped-read alignment with Bowtie 2. Nat Methods. 2012;9(4):357–9.
19. Akalin A, Kormaksson M, Li S, Garrett-Bakelman FE, Figueroa ME, Melnick A, et al. methylKit: a comprehensive R package for the analysis of genome-wide DNA methylation profiles. Genome Biol. 2012;13(10):R87.
20. Wreczycka K, Gosdschan A, Yusuf D, Grüning B, Assenov Y, Akalin A. Strategies for analyzing bisulfite sequencing data. J Biotechnol. 2017;261:105–15.

Kwon *et al. Clinical Epigenetics*   (2025) 17:24

Page 12 of 13

21. Zhang Y, Baheti S, Sun Z. Statistical method evaluation for differentially methylated CpGs in base resolution next-generation DNA sequencing data. Brief Bioinform. 2016;19(3):374–86.

22. Lundberg SM, Erion G, Chen H, DeGrave A, Prutkin JM, Nair B, et al. From local explanations to global understanding with explainable AI for trees. Nature Mach Intell. 2020;2(1):56–67.

23. Cavalcante RG, Sartor MA. annotatr: genomic regions in context. Bioinformatics. 2017;33(15):2381–3.

24. Bindea G, Mlecnik B, Hackl H, Charoentong P, Tosolini M, Kirilovsky A, et al. ClueGO: a Cytoscape plug-in to decipher functionally grouped gene ontology and pathway annotation networks. Bioinformatics. 2009;25(8):1091–3.

25. Ashburner M, Ball CA, Blake JA, Botstein D, Butler H, Cherry JM, et al. Gene ontology: tool for the unification of biology. Nat Genet. 2000;25(1):25–9.

26. Consortium TGO, Aleksander SA, Balhoff J, Carbon S, Cherry JM, Drabkin HJ, et al. The gene ontology knowledgebase in 2023. Genetics. 2023;224(1):iyad031.

27. Kanehisa M, Goto S. KEGG: kyoto encyclopedia of genes and genomes. Nucleic Acids Res. 2000;28(1):27–30.

28. Kanehisa M. Toward understanding the origin and evolution of cellular organisms. Protein Sci. 2019;28(11):1947–51.

29. Kanehisa M, Furumichi M, Sato Y, Kawashima M, Ishiguro-Watanabe M. KEGG for taxonomy-based analysis of pathways and genomes. Nucleic Acids Res. 2023;51(D1):D587–92.

30. Nemesure MD, Heinz MV, Huang R, Jacobson NC. Predictive modeling of depression and anxiety using electronic health records and a novel machine learning approach with artificial intelligence. Sci Rep. 2021;11(1):1980.

31. Chavanne AV, Paillère Martinot ML, Penttilä J, Grimmer Y, Conrod P, Stringaris A, et al. Anxiety onset in adolescents: a machine-learning prediction. Mol Psychiatry. 2023;28(2):639–46.

32. Priya A, Garg S, Tigga NP. Predicting anxiety, depression and stress in modern life using machine learning algorithms. Procedia Comput Sci. 2020;167:1258–67.

33. Bird AP. CpG-rich islands and the function of DNA methylation. Nature. 1986;321(6067):209–13.

34. Antequera F. Structure, function and evolution of CpG island promoters. Cell Mol Life Sci CMLS. 2003;60(8):1647–58.

35. Deaton AM, Bird A. CpG islands and the regulation of transcription. Genes Dev. 2011;25(10):1010–22.

36. Malek M, Wawrzyniak AM, Koch P, Lüchtenborg C, Hessenberger M, Sachsenheimer T, et al. Inositol triphosphate-triggered calcium release blocks lipid exchange at endoplasmic reticulum-Golgi contact sites. Nat Commun. 2021;12(1):2673.

37. Kania E, Roest G, Vervliet T, Parys JB, Bultynck G. IP(3) Receptor-mediated calcium signaling and its role in autophagy in cancer. Front Oncol. 2017;7:140.

38. Prole DL, Taylor CW. Structure and function of IP(3) receptors. Cold Spring Harb Perspect Biol. 2019;11(4): a035063.

39. Song Ba Y, Wang Ma F, Wei Ma Y, Chen Ba D, Deng BG. ATP5A1 participates in transcriptional and posttranscriptional regulation of cancer-associated genes by modulating their expression and alternative splicing profiles in HeLa cells. Technol Cancer Res Treat. 2021;20:15330338211039126.

40. Venesio T, Balsamo A, Errichiello E, Ranzani GN, Risio M. Oxidative DNA damage drives carcinogenesis in MUTYH-associated-polyposis by specific mutations of mitochondrial and MAPK genes. Mod Pathol. 2013;26(10):1371–81.

41. Hwang BJ, Shi G, Lu AL. Mammalian MutY homolog (MYH or MUTYH) protects cells from oxidative DNA damage. DNA Repair (Amst). 2014;13:10–21.

42. Dings MPG, van der Zalm AP, Bootsma S, van Maanen TFJ, Waasdorp C, van den Ende T, et al. Estrogen-related receptor alpha drives mitochondrial biogenesis and resistance to neoadjuvant chemoradiation in esophageal cancer. Cell Rep Med. 2022;3(11): 100802.

43. Huang G, Li H, Zhang H. Abnormal expression of mitochondrial ribosomal proteins and their encoding genes with cell apoptosis and diseases. Int J Mol Sci. 2020;21(22):8879.

44. Shan L, Yang D, Feng F, Zhu D, Li X. miR-3146 induces neutrophil extracellular traps to aggravate gout flare. J Clin Lab Anal. 2021;35(11): e24032.

45. Du J, Chen M, Liu J, Hu P, Guan H, Jiao X. LncRNA F11-AS1 suppresses liver hepatocellular carcinoma progression by competitively binding with miR-3146 to regulate PTEN expression. J Cell Biochem. 2019;120(10):18457–64.

46. Chae HD, Broxmeyer HE. SIRT1 deficiency downregulates PTEN/JNK/FOXO1 pathway to block reactive oxygen species-induced apoptosis in mouse embryonic stem cells. Stem Cells Dev. 2011;20(7):1277–85.

47. Sperandio S, Tardito S, Surzycki A, Latterich M, de Belle I. TOE1 interacts with p53 to modulate its transactivation potential. FEBS Lett. 2009;583(13):2165–70.

48. Shigematsu S, Fukuda S, Nakayama H, Inoue H, Hiasa Y, Onji M, et al. ZNF689 suppresses apoptosis of hepatocellular carcinoma cells through the down-regulation of Bcl-2 family members. Exp Cell Res. 2011;317(13):1851–9.

49. Yi PS, Wu B, Deng DW, Zhang GN, Li JS. Positive expression of ZNF689 indicates poor prognosis of hepatocellular carcinoma. Oncol Lett. 2018;16(4):5122–30.

50. Libert S, Pointer K, Bell EL, Das A, Cohen DE, Asara JM, et al. SIRT1 activates MAO-A in the brain to mediate anxiety and exploratory drive. Cell. 2011;147(7):1459–72.

51. Wang X-Q, Zhang L, Xia Z-Y, Chen J-Y, Fang Y, Ding Y-Q. PTEN in prefrontal cortex is essential in regulating depression-like behaviors in mice. Transl Psychiatry. 2021;11(1):185.

52. Willy PJ, Murray IR, Qian J, Busch BB, Stevens WC, Martin R, et al. Regulation of PPARγ coactivator 1α (PGC-1α) signaling by an estrogen-related receptor α (ERRα) ligand. Proc Natl Acad Sci. 2004;101(24):8912–7.

53. Vanaveski T, Molchanova S, Pham DD, Schäfer A, Pajanoja C, Narvik J, et al. PGC-1α signaling increases GABA(A) receptor subunit α2 expression, GABAergic neurotransmission and anxiety-like behavior in mice. Front Mol Neurosci. 2021;14: 588230. https://doi.org/10.3389/fnmol.2021.588230.

54. Jaka O, Iturria I, van der Toorn M, Hurtado de Mendoza J, Latino D, Alzualde A, et al. Effects of natural monoamine oxidase inhibitors on anxiety-like behavior in zebrafish. Front Pharmacol. 2021;12: 669370. https://doi.org/10.3389/fphar.2021.669370.

55. Bortolato M, Godar SC, Davarian S, Chen K, Shih JC. Behavioral disinhibition and reduced anxiety-like behaviors in monoamine oxidase B-deficient mice. Neuropsychopharmacology. 2009;34(13):2746–57.

56. Cho H-U, Kim S, Sim J, Yang S, An H, Nam M-H, et al. Redefining differential roles of MAO-A in dopamine degradation and MAO-B in tonic GABA synthesis. Exp Mol Med. 2021;53(7):1148–58.

57. Prah A, Purg M, Stare J, Vianello R, Mavri J. How monoamine oxidase a decomposes serotonin: an empirical valence bond simulation of the reactive step. J Phys Chem B. 2020;124(38):8259–65.

58. Bortolato M, Chen K, Shih JC. CHAPTER 24 - The Degradation of Serotonin: Role of MAO. In: Müller CP, Jacobs BL, editors. Handbook of Behavioral Neuroscience. Amsterdam: Elsevier; 2010. p. 203–18.

59. Zanetti G, Pahuja KB, Studer S, Shim S, Schekman R. COPII and the regulation of protein sorting in mammals. Nat Cell Biol. 2012;14(1):20–8.

60. Oo ZM, Adlat S, Sah RK, Myint MZZ, Hayel F, Chen Y, et al. Brain transcriptome study through CRISPR/Cas9 mediated mouse Dip2c gene knockout. Gene. 2020;758: 144975.

61. Shen S, Battersby S, Weaver M, Clark E, Stephens K, Harmar AJ. Refined mapping of the human serotonin transporter (SLC6A4) gene within 17q11 adjacent to the CPD and NF1 genes. Eur J Hum Genet. 2000;8(1):75–8.

62. Mazzanti CM, Lappalainen J, Long JC, Bengel D, Naukkarinen H, Eggert M, et al. Role of the serotonin transporter promoter polymorphism in anxiety-related traits. Arch Gen Psychiatry. 1998;55(10):936–40.

63. Ando K, Erneux C, Homa M, Houben S, de Fisenne M-A, Brion J-P, et al. Dysregulation of phosphoinositide 5-phosphatases and phosphoinositides in alzheimer's disease. Front Neurosci. 2021;15: 614855. https://doi.org/10.3389/fnins.2021.614855.

64. Schachtschneider KM, Welge ME, Auvil LS, Chaki S, Rund LA, Madsen O, et al. Altered hippocampal epigenetic regulation underlying reduced cognitive development in response to early life environmental insults. Genes (Basel). 2020;11(2):162.

65. Martin CA, Vorn R, Schrieber M, Lai C, Yun S, Kim HS, et al. Identification of DNA methylation changes that predict onset of post-traumatic stress disorder and depression following physical trauma. Front Neurosci. 2021;15: 738347.

66. Tao Y, Zhang H, Jin M, Xu H, Zou S, Deng F, et al. Co-expression network of mRNA and DNA methylation in first-episode and drug-naive adolescents

Kwon *et al. Clinical Epigenetics*   (2025) 17:24

Page 13 of 13

with major depressive disorder. Front Psych. 2023;14:1065417. https://doi.org/10.3389/fpsyt.2023.1065417.

67. Snijders C, Maihofer AX, Ratanatharathorn A, Baker DG, Boks MP, Geuze E, et al. Longitudinal epigenome-wide association studies of three male military cohorts reveal multiple CpG sites associated with post-traumatic stress disorder. Clin Epigenetics. 2020;12(1):11.

68. Spindola LM, Santoro ML, Pan PM, Ota VK, Xavier G, Carvalho CM, et al. Detecting multiple differentially methylated CpG sites and regions related to dimensional psychopathology in youths. Clin Epigenetics. 2019;11(1):146.

69. Alisch RS, Chopra P. Blood DNA methylation biomarker diagnostic test for anxiety and depressive disorders. Google Patents; 2023.

70. Moon S, Lee H. JDSNMF: joint deep semi-non-negative matrix factorization for learning integrative representation of molecular signals in alzheimer's disease. J Pers Med. 2021;11(8):686.

71. Krolow R, Arcego DM, Noschang C, Weis SN, Dalmaz C. Oxidative imbalance and anxiety disorders. Curr Neuropharmacol. 2014;12(2):193–204.

72. Fedoce ADG, Ferreira F, Bota RG, Bonet-Costa V, Sun PY, Davies KJA. The role of oxidative stress in anxiety disorder: cause or consequence? Free Radic Res. 2018;52(7):737–50.

73. Tomei LD, Kiecolt-Glaser JK, Kennedy S, Glaser R. Psychological stress and phorbol ester inhibition of radiation-induced apoptosis in human peripheral blood leukocytes. Psychiatry Res. 1990;33(1):59–71.

74. Yin D, Tuthill D, Mufson RA, Shi Y. Chronic restraint stress promotes lymphocyte apoptosis by modulating CD95 expression. J Exp Med. 2000;191(8):1423–8.

75. Segerstrom SC, Miller GE. Psychological stress and the human immune system: a meta-analytic study of 30 years of inquiry. Psychol Bull. 2004;130(4):601–30.

76. Liu Y, Tian S, Ning B, Huang T, Li Y, Wei Y. Stress and cancer: The mechanisms of immune dysregulation and management. Front Immunol. 2022;13:1032294. https://doi.org/10.3389/fimmu.2022.1032294.

77. Holmes A, Murphy DL, Crawley JN. Abnormal behavioral phenotypes of serotonin transporter knockout mice: parallels with human anxiety and depression. Biol Psychiat. 2003;54(10):953–9.

78. Baldwin D, Rudge S. The role of serotonin in depression and anxiety. Int Clin Psychopharmacol. 1995;9:41–6.

79. Lydiard RB. The role of GABA in anxiety disorders. J Clin Psychiatry. 2003;64(Suppl 3):21–7.

80. Kalueff AV, Nutt DJ. Role of GABA in anxiety and depression. Depress Anxiety. 2007;24(7):495–517.

81. Żmudzka E, Sałaciak K, Sapa J, Pytka K. Serotonin receptors in depression and anxiety: insights from animal studies. Life Sci. 2018;210:106–24.

82. Vašíček O, Lojek A, Číž M. Serotonin and its metabolites reduce oxidative stress in murine RAW2647 macrophages and prevent inflammation. J Physiology Biochem. 2020;76(1):49–60.

83. Zhang S, Zhao J, Hu J, He H, Wei Y, Ji L, et al. Gama-aminobutyric acid (GABA) alleviates hepatic inflammation via GABA receptors/TLR4/NF-κB pathways in growing-finishing pigs generated by super-multiparous sows. Anim Nutr. 2022;9:280–90.

84. Wan M, Ding L, Wang D, Han J, Gao P. Serotonin: a potent immune cell modulator in autoimmune diseases. Front Immunol. 2020;11:186. https://doi.org/10.3389/fimmu.2020.00186.

85. Wang YY, Sun SP, Zhu HS, Jiao XQ, Zhong K, Guo YJ, et al. GABA regulates the proliferation and apoptosis of MAC-T cells through the LPS-induced TLR4 signaling pathway. Res Vet Sci. 2018;118:395–402.

86. Khanzode SD, Dakhale GN, Khanzode SS, Saoji A, Palasodkar R. Oxidative damage and major depression: the potential antioxidant action of selective serotonin re-uptake inhibitors. Redox Rep. 2003;8(6):365–70.

87. Zhang FF, Cardarelli R, Carroll J, Fulda KG, Kaur M, Gonzalez K, et al. Significant differences in global genomic DNA methylation by gender and race/ethnicity in peripheral blood. Epigenetics. 2011;6(5):623–9.

88. Kader F, Ghai M. DNA methylation-based variation between human populations. Mol Genet Genomics. 2017;292(1):5–35.

89. Jones MJ, Goodman SJ, Kobor MS. DNA methylation and healthy human aging. Aging Cell. 2015;14(6):924–32.

Publisher's Note